

Article

The Influences of Stirring on the Recrystallization of Ammonium Perrhenate

Junjie Tang^{1,2,3,*}, Li Feng⁴, Chunwei Zhang^{3,5}, Yuan Sun^{3,*}, Long Wang³, Yizhou Zhou^{3,*}, Dawei Fang⁵ and Yan Liu²

¹ School of Biomedical & Chemical Engineering, Liaoning Institute of Science and Technology, Benxi 117004, China

² Key Laboratory for Ecological Utilization of Multimetallic Mineral, Ministry of Education, Northeastern University, Shenyang 110819, China; liuyan@smm.neu.edu.cn

³ Institute of Metal Research, Chinese Academy of Sciences, Shenyang 110016, China; 13842034917@163.com (C.Z.); wanglong@imr.ac.cn (L.W.)

⁴ Electrical engineering, Shenyang Polytechnic College, Shenyang 110045, China; lifeng@163.com

⁵ College of chemistry, Liaoning University, Shenyang 110036, China; davidfine@163.com

* Correspondence: tangjunjieyh@lnist.edu.cn (J.T.); yuansun@imr.ac.cn (Y.S.); yzzhou@imr.ac.cn (Y.Z.); Tel.: +86-024-2397-1767 (J.T.); +86-024-2397-1767 (Y.S.); +86-024-8397-8068 (Y.Z.)

Received: 16 December 2019; Accepted: 13 January 2020; Published: 16 January 2020



Featured Application: This study provides a theoretical basis and practical experience for optimizing the recrystallization process of ammonium perrhenate and the design of a recrystallization reactor.

Abstract: Ammonium perrhenate is widely used in alloy manufacturing, powder processing, the catalytic industry, and other fields. Recrystallization can improve the specific surface area of ammonium perrhenate, reduce its particle size, and improve its particle size distribution uniformity. Therefore, recrystallized ammonium perrhenate can obtain better application benefits in the above fields. Stirring is an important factor that affects the recrystallization of ammonium perrhenate, and this paper systematically analyzes the influence of the stirring paddle types and stirring intensities on ammonium perrhenate during the homogeneous recrystallization process, ultimately revealing the relationship between the growth rate of ammonium perrhenate and the stirring process. Particle image velocimetry physical simulation results showed that the flow field in the reactor was more evenly distributed when using the disc turbine impeller, and a relatively uniform velocity liquid flow area was formed in the whole reactor, while the low-velocity liquid flow area was smaller. Therefore, this information, combined with SEM test results, suggests that under the same recrystallization time and stirring intensity, the stirring effect of a disc turbine impeller is more suitable than a propelling propeller and an Intermig impeller for the recrystallization process of ammonium perrhenate. Moreover, the XRD patterns and SEM analysis showed that if the agglomeration in the systems was too strong or too weak, the growths of the (101) crystal plane and (112) crystal plane were restrained, which caused an attenuation in the growth rates along the crystallographic directions that were orthogonal to the crystal faces. Finally, the reduction experiments show that the recrystallization of ammonium perrhenate could improve the phase parameters of rhenium powders.

Keywords: ammonium perrhenate; recrystallization; stirring paddle type; agglomeration

1. Introduction

As an important strategic rare metal, Re is widely used in the metallurgy, chemical, alloy manufacturing and aerospace industries [1,2]. At present, the preparation technologies for Re include

plasma methods, electrolysis methods, vapor deposition methods, and the hydrogen reduction of ammonium perrhenate [3,4]. Rhenium powders have the advantages of excellent phase parameters and uniform particle size distribution when prepared by electrolysis, vapor deposition, and plasma methods. Jerzy W. Jurewicz et al. [5] produced micro/nano rhenium powders by applying the plasma method. T. Leonhardt et al. [6] carried out the plasma spray spheroidization of rhenium powders produced by traditional processes and obtained spherical rhenium powders with microscopic morphologies. R. Schrebler et al. [7] used a mixed solution of rhenic acid and sodium sulfate as electrolytes to produce spherical rhenium powders by electrolysis. Zhihong Liu et al. [8] produced spherical ultrafine rhenium powders with a small particle size by using the vapor deposition method. However, due to the complex equipment and the difficulties in process scale up, none of the above preparation processes have achieved large-scale production.

The preparation of Re by the hydrogen reduction of ammonium perrhenate is the only industrial production process and has the advantages of straightforward operation, low production cost, and uncomplicated equipment [9]. However, there are still some problems to be solved with this preparation method. The rhenium powders are produced with an uneven particle size distribution and poor powder phase parameters. These powders cause difficulties during subsequent application and processing and cannot meet the high requirements for powders that are used for modern powder metallurgy fabrication methods [10]. These issues are mainly caused by the low efficiency of the mass transfer and heat transfer during the reduction process of ammonium perrhenate. Some scholars have made progress with the reduction control of metal powders. For instance, Qiuping Liu et al. [11] improved the particle uniformity of molybdenum powder by controlling heat release. Guodong Sun et al. [12] studied the growth of molybdenum powder when the particle size was controlled by adding NaCl. Hyunji Kang et al. [13] prepared nanometer tungsten powder by applying a ball milling pretreatment of WO_3 . All of the above studies aimed to improve the phase parameters and uniformity of the powder by improving its mass transfer and heat transfer efficiency by relying on the pretreatment of the reducing substances. Therefore, previous studies have shown that optimizing the phase parameters of ammonium perrhenate can affect the phase parameters of reduction products. Ammonium perrhenate is purified by recrystallization in industrial contexts [14]. The static cooling recrystallization process produces ammonium perrhenate with a large particle size, uneven particle size distribution, and serious particle agglomeration. Tianrong Cao et al. [15] prepared $Ni(OH)_2$ with uniform particle size distribution by airlift-loop and stirred reactors. Wei Jia [16] changed the size of the crystals by optimizing the structure of the stirred reactor. In conclusion, previous studies have provided references for improving the process of preparing rhenium powders by using the hydrogen reduction of ammonium perrhenate.

The aim of the present study was to enhance the mass and heat transfer efficiency of ammonium perrhenate during the reduction process by relying on a homogeneous recrystallization reduction pretreatment to improve the uniformity and specific surface of the ammonium perrhenate. The influence of stirring paddle types and stirring intensities on the phase parameters during the recrystallization of ammonium rhenate is systematically explored, and the growth mechanism during ammonium perrhenate recrystallization is revealed. Then, the flow field distribution in the reactor under different stirring intensities and agitator types is simulated by PIV (particle image velocimetry) physical model technology, and the recrystallization process of ammonium perrhenate is described from the flow field viewpoint. This study provides a theoretical basis and practical experience for optimizing the recrystallization process of ammonium perrhenate and the design of a recrystallization reactor.

2. Materials and Methods

2.1. Instrument

Instruments: Quintix224-1CN electronic balance, Xiang Yi Company, China; RE-2000A rotary evaporator, Yi Jie Science Company, Beijing, China; SSX-550 scanning electron microscope, Shimadzu,

Japan; PW3040/60 X-ray diffractometer, Panalytical Company, EA Almelo, The Netherlands; high-temperature vacuum sintering furnace, Zhuzhou Guangjichang Technology Company, Zhuzhou, China; 3H-2000BET-A specific surface area tester, Best instrument co. LTD, Beijing, China; BT9300S laser particle size analyzer, Bettersize instruments co. LTD, Dandong, China; Self-designed recrystallization condensation reactor; Particle image velocimetry system, two dimensional particle velocity meters, Dantec co. LTD, Skovlunde, Denmark.

2.2. Materials

Materials: NH_4ReO_4 (99.99%, Re \geq 69.4%) Halin Chemical Co. LTD, Weifang, China. The scanning electron microscopy (SEM) of the NH_4ReO_4 raw material is shown in Figure 1.

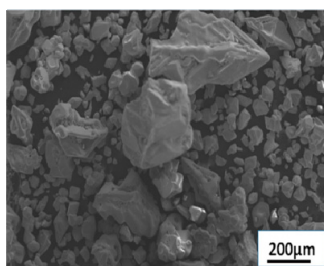


Figure 1. The SEM of NH_4ReO_4 raw materials.

2.3. Analytical Methods

XRD detection: The light tube type was a Cu target, ceramic X light tube. $\lambda = 0.15406$ nm, the scan range was 10~90 degrees, and the scanning speed was 2 degrees/min.

Particle size distribution detection: The test medium was ethanol, the optical model was Mie, and the distribution type was volume distribution.

The flow field distribution processing software was Tecplot.360.v11.0.1 from Tecplot co. LTD, Bellevue, WA, USA.

The parameters of SEM:

- (1) Low power imaging: The electron acceleration voltage was 20.0 KV, the working distance was 9.5 mm, and the magnification was 100 times.
- (2) High power imaging: The electron acceleration voltage was 20.0 KV, the working distance was 9.5 mm, and the magnification was 800 times.

Physical simulation analysis method:

- (1) Design of water model: In this study, a 1 L self-designed recrystallization condensation reactor was taken as the prototype, and the water model was established based on the similarity principle (geometric similarity). The water model and prototype met the following conditions: $N_2 = N_1(T_1/T_2) \times$ (Formula (1)), T_1 was the inner diameter of the water model, T_2 was the inner diameter of the prototype reactor, N_1 was the stirring intensity (rpm) of the water model, and N_2 was the stirring intensity (rpm) of the prototype reactor. X was the amplification index. $X = 1$ means that the linear stirring speeds of geometrically similar reactors were the same [17]. The inner diameter of the recrystallization condensation reactor was 140 mm. According to the principle of geometric similarity, the water model of the recrystallization condensation reactor was established. The inner diameter of the water model was 240 mm. The volume ratio of the water model to the prototype is 5:1.
- (2) Procedures of physical simulation: According to Formula (1), when the stirring speed of the recrystallization condensation reactor was 200 rpm, the stirring speed of the water model was about 120 rpm. The right amount of tracer particles (polystyrene) was added into the water, and then the particle image velocimetry two dimensional particle velocity meter was turned on.

After the computer received the image data, Tecplot.360.v11.0.1 software was used for processing to get the vector images.

2.4. Experimental Procedure

- (1) The sample preparation of ammonium perrhenate: The NH_4ReO_4 raw material was dissolved in deionized water to form a supersaturated solution at room temperature (25 °C). The NH_4ReO_4 solution was then evaporated to the RE-2000A rotary evaporator (oil bath temperature 120 °C) and formed the supersaturated solution at a high temperature [18]. The hot supersaturated solution was passed into the recrystallization condensation reactor, the stirring strength of the reactor was adjusted to cool during crystallization, the recrystallization time was 3 h, the recrystallized solid–liquid mixtures were filtered by the vacuum filter extractor, the solid samples were obtained and dried prior in the oven to being measured, and the oven temperature was 60 °C. The ammonium perrhenate samples in this paper were prepared at the stirring strengths of 100, 150, 200 and 250 rpm.
- (2) Sample preparation of rhenium powders: In this paper, non-recrystallized ammonium perrhenate (as shown in Figure 1) and recrystallized ammonium perrhenate at a 200 rpm (the disc turbine impeller was used) stirring strength were used as raw materials to prepare the rhenium powder samples. The two kinds of ammonium perrhenate particles (60 g) were reduced with the same reduced time (3 h) in the high-temperature vacuum sintering furnace, and the reduced samples were obtained. The hydrogen flow rate was 500 mL/min. The heating rate was 10 °C/min.

3. Results

3.1. The Influences of Paddle Types

Three kinds of stirring paddles that are commonly used in industry were studied in this study, which were the disc turbine impeller, the propelling propeller, and the Intermig impeller. The diagrams of the stirring paddles are shown in Figure 2. Under the same recrystallization time and agitation intensity (200 rpm), SEM images of the NH_4ReO_4 crystals prepared in the prototype reactor with different stirring paddle types are shown in Figure 3. It can be seen that the morphologies of most crystal particles that were prepared by the disc turbine impeller were regular, the crystal surfaces were smooth, and a few crystal particles had rough surfaces, indicating that most crystal particle development was relatively complete. The crystal particle with a high magnification was the representative of the complete growth of the crystal particles. However, the morphologies of most crystal particles prepared by the propelling propeller and the Intermig impeller had uneven surface topographies, indicating that the crystals were not fully developed. The crystal particles with a high magnification were the representative of the incomplete growth crystal particles. This suggests that under the same operating conditions, the stirring effect of the disc turbine impeller is more suitable for the homogeneous recrystallization process.

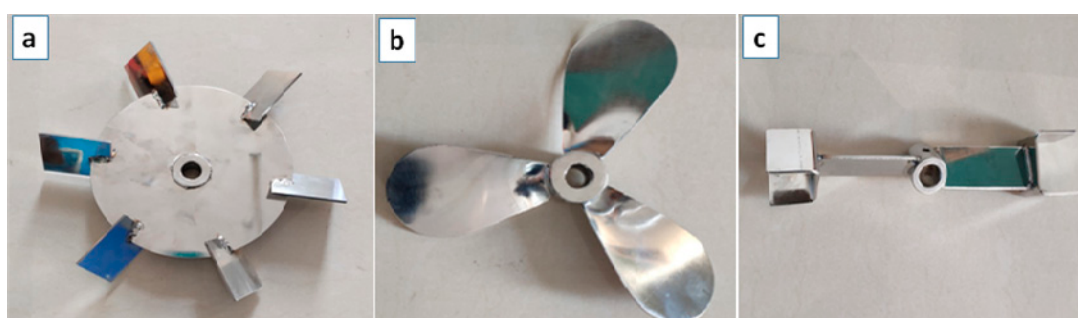


Figure 2. The diagram of the water model (a—disc turbine impeller; b—propelling propeller; and c—Intermig impeller).

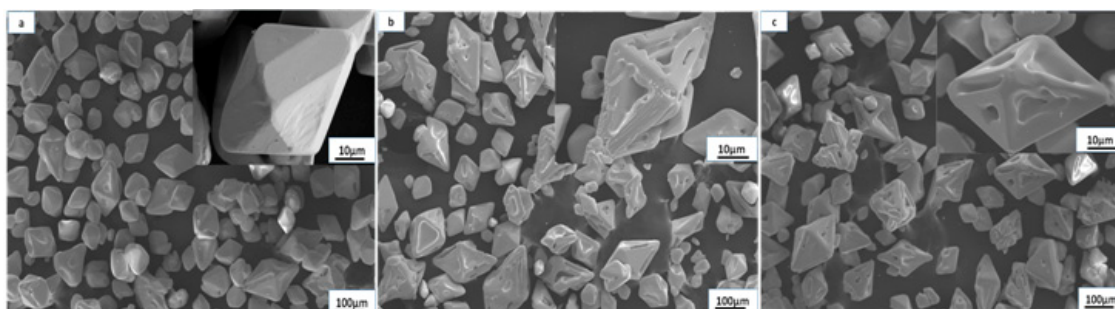


Figure 3. SEM images of the NH_4ReO_4 particles with different stirring paddle types (a—disc turbine impeller; b—propelling propeller; and c—Intermig impeller).

3.2. The Influences of Stirring Intensities

An ammonium perrhenate crystal is tetragonal 4/m (isostructural with the scheelite CaWO_4), and it is a typical form of monometric crystals [19]. The crystals were in solution, and the growth process of the crystals ended when the solute was precipitated and dissolved in equilibrium [20]. To inspect the effect of the agitation intensities on the crystal morphologies, the SEM micrographs of the NH_4ReO_4 samples with different agitation intensities (the disc turbine impeller was used) are shown in Figure 4. When the agitation intensity was 100 rpm, many irregularly shaped crystals with different sizes were formed when the crystalline system was in equilibrium; the surface structures of these crystals were rough and uneven, as shown in Figure 4a. Crystals with irregular morphologies are generally considered to be underdeveloped [21,22]. This suggests that the strong crystal agglomeration effect led to incomplete crystal development during equilibrium with the dissolved solute. When the agitation intensity was 150 rpm, the macroscopic morphologies of these crystals were mostly tetragonal crystals, and the surfaces of these crystals were defective and smooth, as shown in Figure 4b. It can be seen that the crystal agglomeration effect was subdued at high stirring speeds, the uniformity of the crystals increased, the crystal morphologies became regular, and, when the crystal system was in equilibrium, the morphologies of the crystals were more regular. When the agitation intensity was 200 rpm, the NH_4ReO_4 particles formed tetragonal crystals with a similar morphologies and sizes, and the surfaces of these crystals were neat and smooth, as shown in Figure 4c. This suggests that when the crystal agglomeration effect was further weakened, the morphologies of the crystals were further improved when in equilibrium with the crystal system. When the agitation intensity was 250 rpm, the macroscopic morphologies of these crystals were mostly tetragonal crystals. However, there were small crystals that could be found, and the surfaces of these crystals were defective and smooth, as shown in Figure 4d. This suggests that when the crystal agglomeration effect was excessively weakened, the integrity of crystal morphologies deteriorated when in equilibrium with the crystal system, and the crystal surface morphologies had obvious defects.

The specific surfaces and D_{50s} (median diameter) of the NH_4ReO_4 samples with different agitation intensities are given in Table 1. It can be seen that as the stirring speeds increased, the specific surfaces and the D_{50} decreased. When the stirring speeds were higher than 200 rpm, the specific surface began to decrease and the D_{50} began to increase. The purpose of this work was to reduce the size of ammonium perrhenate and enhance its specific surface area. Therefore, it was determined that 200 rpm was an ideal recrystallization condition. Therefore, the stirring speeds above 200 rpm had no significance.

In order to research the relationship between the difference of crystal morphologies and the selectivity of crystal growth directions, XRD analyses were performed. The XRD patterns of the samples at different stirring speeds and the same crystallization time (2 h) are shown in Figure 5, and the XRD information is given in Table 2.

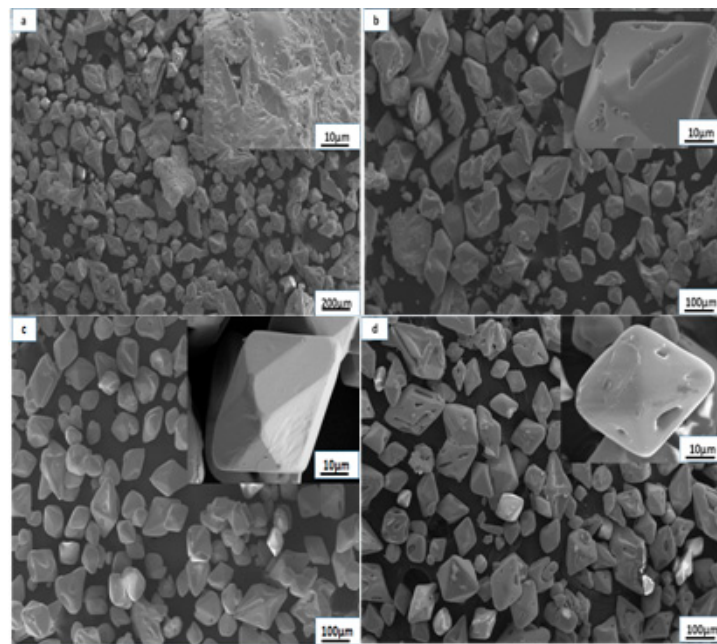


Figure 4. SEM images of the NH_4ReO_4 recrystallization particles at different agitation intensities (a—100 rpm; b—150 rpm; c—200 rpm; and d—250 rpm).

Table 1. Specific surfaces and D50s (median diameter) of the samples at different stirring speeds.

Agitation Intensity (rpm)	Specific Surface (m^2/kg)	D50 (μm)
100	21.72	81.05
150	24.56	79.32
200	26.93	71.17
250	23.54	78.97

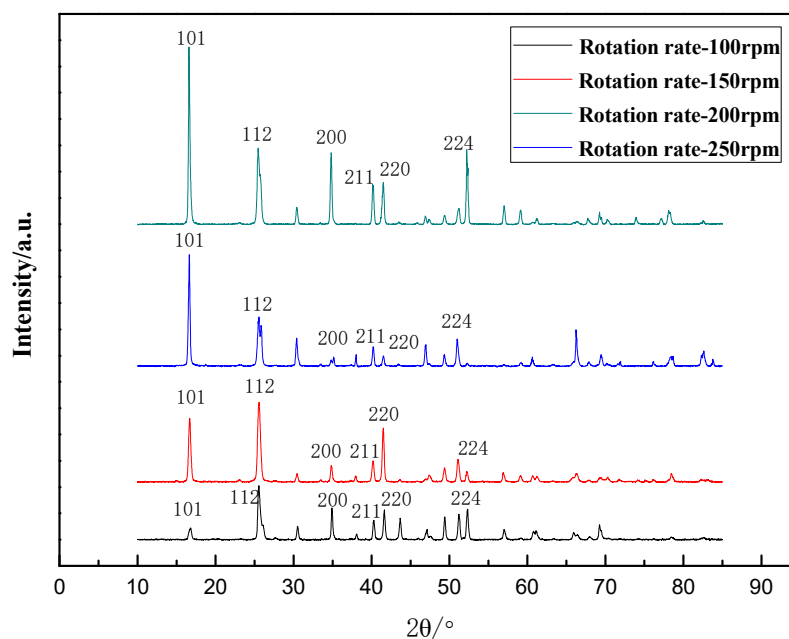


Figure 5. XRD patterns of the NH_4ReO_4 recrystallization particles at different stirring speeds.

Table 2. XRD information of the NH_4ReO_4 recrystallization particles at different stirring speeds.

Agitation Intensity (rpm)	FWHM [$101^\circ 2\theta$.]	FWHM [$112^\circ 2\theta$.]	D(nm) [$101^\circ 2\theta$.]	D(nm) [$112^\circ 2\theta$.]
100	0.2558	0.2755	0.5575	0.5536
150	0.2165	0.2165	0.6587	0.7045
200	0.1574	0.1771	0.9061	0.8613
250	0.1968	0.2558	0.7247	0.5963

The diffraction peaks were from the NH_4ReO_4 , and other crystalline species were not observed. These diffraction peaks had different intensities. When the stirring intensity was 200 rpm, the diffraction peaks had the strongest intensities. This indicated that when the stirring intensity was 200 rpm, the selective growth rates of the crystal planes corresponding to the characteristic peaks were higher than that of other samples. In this paper, the selectivity of the crystal growth directions on the (101) crystal planes and (112) crystal planes at different stirring speeds could be calculated by the Scherrer formula, where $D = K\lambda / (B \cos \theta)$; the results are given in Table 3. Table 3 shows that the growth rates of the (101) crystal planes and (112) crystal planes were promoted with increasing stirring speeds (100~200 rpm). However, the growth rates of the (101) crystal planes and (112) crystal planes were subdued at the excessive stirring speed (250 rpm).

Table 3. Selectivity of crystal growth directions for NH_4ReO_4 at different stirring speeds.

Crystal Planes	Agitation Intensity (rpm)	D (nm)
(101)	100	0.5575
	150	0.6587
	200	0.9061
	250	0.7247
(112)	100	0.5536
	150	0.7045
	200	0.8613
	250	0.5963

3.3. Reduction Experimental

In this study, the recrystallized NH_4ReO_4 crystals were prepared at 200 rpm, and the NH_4ReO_4 crystals without recrystallization (NH_4ReO_4 (99.99%, Re \geq 69.4%) Halin Chemical Co. LTD, Weifang, China.) were reduced by H_2 at high temperatures. The full reduction temperature of the recrystallized NH_4ReO_4 crystals was at 700 °C, while the full reduction temperature of the NH_4ReO_4 without recrystallization crystals was at 1000 °C. Moreover, the rhenium powders that were prepared by recrystallized NH_4ReO_4 crystals had a very even size distribution, as shown in Figure 6b. However, the rhenium powders that were prepared by the NH_4ReO_4 crystals without recrystallization had an uneven particle size distribution, as shown in Figure 6a. The rhenium powders that were prepared by recrystallized NH_4ReO_4 crystals had smaller D_{50} s and larger specific surfaces, as shown in Table 4. This shows that the Re powders that were prepared by recrystallized ammonium rhenate had a more uniform particle size distribution, a smaller D_{50} , and a larger specific surface area.

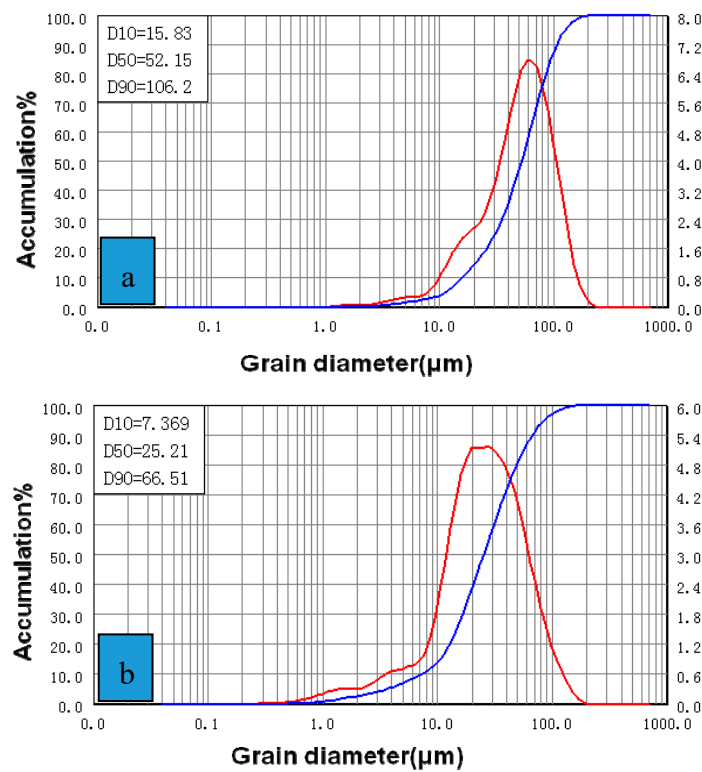


Figure 6. Particle size distribution of the rhenium samples. **a**—Sample was prepared with the NH_4ReO_4 crystals without recrystallization. **b**—Sample was prepared by the recrystallization NH_4ReO_4 crystals at 200 rpm. The red line represents particle size (μm), and the blue line represents the accumulation.

Table 4. Specific surfaces and D50s of the rhenium powders.

Re Powders	D50 (μm)	Specific Surface (m^2/kg)	Reduction Temperature ($^\circ\text{C}$)
Preparation of NH_4ReO_4 without recrystallization	42.16	105.80	1000
Preparation of recrystallization NH_4ReO_4	25.21	182.10	700

4. Discussion

In order to study the effects of agitator types on recrystallization, PIV physical simulation technique was used to simulate the flow field distribution in the reactor. The velocity vector cloud diagrams of the flow field distribution with different agitator types at the same agitator speed and agitator position are shown in Figure 7. It can be seen that the flow field in the reactor was more evenly distributed when using the disc turbine impeller, and a relatively uniform velocity liquid flow area was formed in the whole reactor while the low-velocity liquid flow area was smaller, as shown in Figure 7a. When the Intermig impeller was used, the high-speed liquid flow area was mainly distributed at both sides of the agitator shaft and at the bottom of the reactor. However, the other areas of the reactor belonged to the low-speed liquid flow zone, and the flow field was not evenly distributed, as shown in Figure 7b. When the propelling propeller was used, two high-speed circulating liquid flow zones were formed on both sides of the agitator, and the high-speed liquid flow zone was mainly distributed on both sides of the bottom of the reactor. However, the other areas of the reactor belonged to the low-speed liquid flow zone, and the flow field was not evenly distributed, as shown in Figure 7c. In conclusion, the distribution of flow field in the reactor was more uniform when the disc turbine impeller was used, and the relatively low-speed flow area of the reactor was smaller. Combined with the SEM test results (Figure 3), this suggests that under the uniform flow field, the large particles collided and broke into the small particles of uniform size, and then these particles became nuclei again and grew into

complete crystals under uniform flow. Therefore, the stirring effect of the disc turbine impeller is more suitable for the homogeneous recrystallization process.

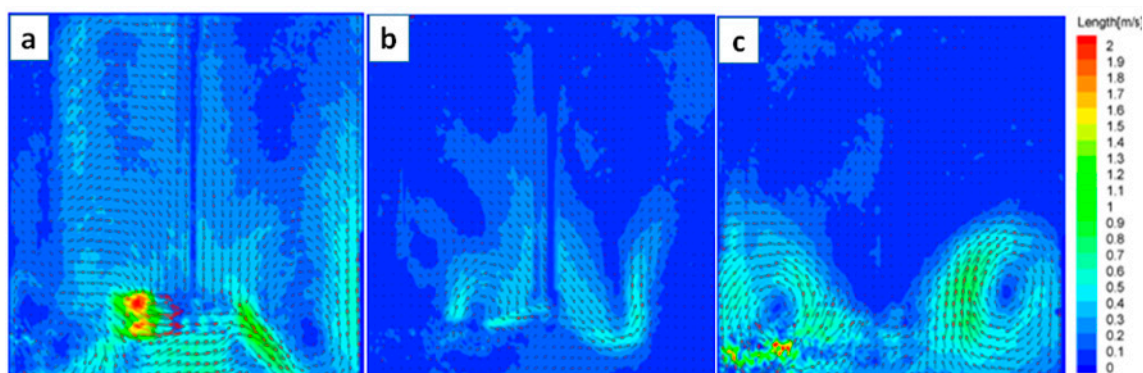


Figure 7. The velocity vector cloud diagrams of flow field distribution with different agitator types (a—disc turbine impeller; b—Intermig impeller; and c—propelling propeller).

As discussed above, the recrystallization of ammonium perrhenate was accompanied by agglomeration, and appropriately increasing the stirring intensity reduced the agglomeration effect. The SEM and XRD analyses showed that an appropriate reduction of the agglomeration effect was conducive to increasing the growth rates of the ammonium perrhenate crystals. When the stirring intensity was 200 rpm, the growth rates of the (101) and (112) crystal planes corresponding to the characteristic peaks of the crystals were relatively fast, as shown in Table 3. Therefore, the crystal development was more complete at the same crystallization time. However, when the stirring intensity was 250 rpm, the agglomeration of the system was excessively reduced; the growth rates of the (101) and (112) crystal planes corresponding to the characteristic peaks of the crystals were subdued, resulting in a slow and incomplete crystal development. This suggested that the induction period for nucleation was reduced and the formation of crystal nuclei and growth of crystals reached an ideal equilibrium state when an appropriate reduction in the agglomeration was obtained. The high stirring intensity also made the large sedimentary particles collide, transition into the secondary crystallization stage, and maintain a uniform grain size in the crystal. However, the excessive stirring intensity enhanced the collisions between the particles, and the agglomeration was excessively weakened. Therefore, the excessive stirring intensity broke the balance for the nucleation process; the generated crystal nuclei collided and broke up under the excessive stirring intensity, resulting in a decrease of the number of crystal nuclei and an increase of the grain size, ultimately leading to an unsatisfactory crystal development. Moreover, the experimental reduction showed that the recrystallized ammonium perrhenate had a better mass and heat transfer efficiency, and it was more conducive to obtain a rhenium powder with more uniform particle size distribution and a larger specific surface area during hydrogen reduction.

5. Conclusions

In this study, the process control of the homogeneous recrystallization of ammonium perrhenate was investigated. According to the results of the present research, the conclusions are as follows:

- (1) The distribution of flow field in the reactor was more uniform and the relatively low-speed flow area of the reactor was smaller when the disc turbine impeller was used, and the disc turbine impeller was more suitable for the ammonium perrhenate recrystallization process.
- (2) The proper reduction of the agglomeration effect was conducive to increasing the growth rates of the ammonium perrhenate crystals, and the growth rates of the (101) crystal planes and (112) crystal planes were promoted with increasing stirring speeds (100~200 rpm). However, the

growth rates of the (101) crystal planes and (112) crystal planes were subdued at the excessive stirring speed (250 rpm).

- (3) The recrystallized ammonium perrhenate had a better mass and heat transfer efficiency, and it was more conducive to obtain the rhenium powder with a more uniform particle size distribution and a larger specific surface area during hydrogen reduction.

Author Contributions: J.T. and C.Z. performed the experiments and tests. J.T., Y.S. and Y.Z. analyzed the results. J.T. and Y.S. designed the experiments. J.T., L.W., D.F. and Y.L. wrote the manuscript. Y.L. and L.F. provided help in revising this article. All authors have read and agreed to the published version of the manuscript.

Funding: This research was funded by open project fund of key laboratory of ecological metallurgy of polymetallic symbiosis in ministry of education, Northeastern University, grant number NEMM2019003; Liaoning provincial department of science and technology doctoral research initiation fund, grant number 2019-BS-130.

Acknowledgments: This work was financially supported by open project fund of key laboratory of ecological metallurgy of polymetallic symbiosis in ministry of education, Northeastern University and Liaoning provincial department of science and technology doctoral research initiation fund, grant number 2019-BS-130. The authors are grateful for these supports.

Conflicts of Interest: The authors declare no conflict of interest.

References

- Li, L.P.; Liu, Y.; Zhang, W.; Jiang, L.J.; Zhang, W.Z. Recent Development of Rhenium Technology. *China Molybdenum Ind.* **2016**, *40*, 1–6.
- Yu, C.; Chen, S.Q.; Li, Y.; Liu, Q.Y. Discussion of World and China Rhenium Resource Demand in 2030. *China Min. Mag.* **2014**, *23*, 9–11, 29.
- Li, H.M.; He, X.T.; Zhou, Y.; Guo, J.M.; Han, S.L.; Wang, H.; Li, Y.; Tan, M.L. Resources, Application and Extraction Status of Rhenium. *Precious Met.* **2014**, *35*, 77–81.
- Noar, A.; Eliaz, N.; Gileadi, E.; Taylor, S.R. Properties and applications of rhenium and its alloys. *Ammtiac Q.* **2010**, *5*, 11–14.
- Jurewicz, J.W.; Guo, J.Y. Process for Plasma Synthesis of Rhenium Nano and Micro Powders, and for Coating and New Net Shape Deposits Thereof and Apparatus Therefor. U.S. Patent 2005/0211018A1, 29 September 2005.
- Leonhardt, T.; Trybus, C.; Hickman, R. Consolidation Methods for Spherical Rhenium and Rhenium Alloys. *Powder Metall.* **2003**, *46*, 148–153. [[CrossRef](#)]
- Schrebler, R.; Cury, P.; Orellana, M.; Gómez, H.; Córdova, R.; Dalchiale, E.A. Electrochemical and Nanoelectrogravimetric Studies of the Nucleation and Growth Mechanisms of Rhenium on Polycrystalline Gold Electrode. *Electrochim. Acta* **2001**, *46*, 4309–4318. [[CrossRef](#)]
- Liu, Z.H.; Zhang, S.Y.; Liu, Z.Y.; Li, Y.H.; Wang, J. Principle and Research Development of Powder Materials Prepared by Chemical Vapor Deposition. *Mater. Sci. Eng. Powder Metall.* **2009**, *14*, 359–364.
- Zhou, L.J.; Bai, M.; Liu, Z.H.; Liu, Z.Y.; Li, Q.H.; Zhang, C.F. The Effect of Sintering on the Properties of Ultrafine Rhenium Powders Prepared by CVD Method. *Rare Met. Mater. Eng.* **2011**, *40*, 1699–1702.
- Zan, L.H.; Yang, B.; Wang, Y.H.; Zhao, J.C.; Fan, X.X. Preparation of Ultrafine Cobalt Powder by Hydrogen Reduction. *J. Mater. Sci. Eng.* **2010**, *28*, 571–575.
- Liu, Q.P.; Bai, Y.; Yi, S.F.; An, P.F. The Effect of Hydrogen Dew Point on the Properties of Molybdenum Dioxide and Molybdenum Powder. *China Tungsten Ind.* **2018**, *33*, 42–46.
- Sun, G.D.; Wang, K.F.; Ji, X.P.; Liu, J.K.; Zhang, H.; Zhang, G.H. Preparation of ultrafine/nano Mo particles via NaCl-assisted hydrogen reduction of different-sized MoO₂ powders. *Int. J. Refract. Met. Hard Mater.* **2019**, *80*, 243–252. [[CrossRef](#)]
- Kang, H.J.; Jeong, Y.K.; Oh, S.T. Hydrogen reduction behavior and microstructural characteristics of WO₃ and WO₃-NiO powders. *Int. J. Refract. Met. Hard Mater.* **2019**, *80*, 69–72. [[CrossRef](#)]
- Zhou, F.Y. Preparation of High Purity Ammonium Perrhenate Process Research. *Copp. Eng.* **2016**, *6*, 56–59.
- Cao, T.R.; Zhang, W.P.; Chen, J.C.; Yang, C. Comparative experimental study on reactive crystallization of Ni(OH)₂ in an airlift-loop reactor and a stirred reactor. *Chin. J. Chem. Eng.* **2018**, *1*, 196–206. [[CrossRef](#)]
- Jia, W. *Optimization of Crystallizer with Draft Tube*; Beijing University of Chemical Technology: Beijing, China, 2014.

17. Chen, Z.P.; Zang, X.W.; Lin, X.H. *Mixing and Mixing Equipment Design and Selection Manual*, 1st ed.; Chemical Industry Press: Beijing, China, 2004; pp. 88–89.
18. Tang, J.J.; Sun, Y.; Hou, G.C.; Ding, Y.T.; H, F.W.; Zhou, Y.Z. Studies on Influencing Factors of Ammonium Rhenate Recovery from Waste Superalloy. *Appl. Sci.* **2018**, *8*, 2016. [[CrossRef](#)]
19. Swainson, P.; Brown, R.J.C. Refinement of Ammonium Perrhenate Structure Using a Pseudo-Spin Model for the Ammonium Ion Orientation. *Acta Cryst.* **1997**, *53*, 76–78. [[CrossRef](#)]
20. Xu, G.; Li, Y.J.; Gu, Z.; Nan, R.H.; Feng, X.Y. Growth and Phase Transformation of Metastable β - HgI_2^{M} . *Chin. J. Inorg. Chem.* **2016**, *32*, 1135–1140.
21. Tang, J.J.; Liu, Y.; Tian, L.; Wang, D.X.; Zhang, T.A. The influence of flow field distribution on the crystallization of spherical nickel hydroxide in reactor. *Chin. J. Inorg. Chem.* **2016**, *32*, 1127–1134.
22. Tang, J.J.; Li, Y.J.; Tian, L.; Zhang, L.L.; Wang, D.X.; Zhang, T.A. The influence of crystal growth direction selectivity on morphology and electrochemical activity of spherical nickel hydroxide. *Chin. J. Inorg. Chem.* **2017**, *32*, 354–360.



© 2020 by the authors. Licensee MDPI, Basel, Switzerland. This article is an open access article distributed under the terms and conditions of the Creative Commons Attribution (CC BY) license (<http://creativecommons.org/licenses/by/4.0/>).